Evolution of the Chemical and Morphological Changes of HDPE When Subjected to Digestion in a Strong Acid Medium

F. Avalos-Belmontes,[1] J. C. Ortiz-Cisneros,[1] I. Zapata-Gonzalez,[1] S. Sánchez-Valdes,[2] L. F. Ramos-deValle[2]

[1]*Facultad de Ciencias Químicas, (FCQ) Universidad Autónoma de Coahuila (UAdeC), Ave. V. Carranza S.N., 25000 Saltillo, Coahuila, México*
[2]*Centro de Investigación en Química Aplicada (CIQA), Blvd. Enrique Reyna 140, 25253 Saltillo, Coahuila, México*

Received 9 June 2010; accepted 30 March 2011
DOI 10.1002/app.34590
Published online 7 September 2011 in Wiley Online Library (wileyonlinelibrary.com).

ABSTRACT: High-density polyethylene (HDPE) is the polymer most used for geomembranes, and one of the tests to determine its applicability is its long term resistance to oxidation. In this sense, this work focuses on the study of the chemical and morphological changes that PE films may experiment when subjected to digestion in nitric acid, simulating the severe ambient conditions of a landfill. The effect of digestion of HDPE, on its chemical and morphological structure, was evaluated. It was observed that the molecular weight of HDPE decreases, forming acid and nitro groups, as the time of digestion increases. Also, the oxidative degradation first produced a bimodal MW distribution, but as the time of strong acid treatment increases, a trimodal MW distribution appears, at lower molecular weights. Finally, as time of digestion continued, a bimodal MW distribution appears again, but at much lower molecular weights. The crystal size of the treated HDPE is directly related to the HDPE molecular weight, that is, as time of digestion increases, the molecular weight decreases and the crystal size decreases. In addition, the heterogeneity of molecular weights, such as bimodal and trimodal distributions, and the presence of chemical groups other than the normal —CH_2— strings of pure PE produced defects in the unit cell parameters **a** and **b**. © 2011 Wiley Periodicals, Inc. J Appl Polym Sci 123: 3248–3254, 2012

Key words: selective extraction; crystallinity; thermo-oxidative degradation; geomembranes

INTRODUCTION

A very interesting application of synthetic geomembranes is in ascertaining the secure disposition of industrial and municipal wastes. These geomembranes will form a barrier and impede the permeation of potentially harmful products and avoid the contamination of the groundwater.

The main materials used for the synthesis of these geomembranes are the polyolefins, whose chemistry and semicrystallinity impart to them the good chemical and mechanical properties necessary to assure the extended life of these geomembranes in this applications.

The most used polymers for the preparation of these geomembranes are usually polyolefins. High-density polyethylene (HDPE) films are the preferred in landfill applications[1] and generally they are available in various thicknesses ranging from 1 to 3 mm. For hazardous waste, film thicknesses may range from 2 to 3 mm, whereas for municipal waste, these may range from 1 to 2.5 mm.

They are applied in the form of a film at the base of a dumping site and act as an insulating layer between the waste and the soil. Nonetheless, it is known that in some cases, the residues carry very corrosive substances which in contact with the geomembrane can attack it and alter its composition and structure. In such a case, its chemical and mechanical properties can be reduced drastically, presenting the risk of leakage, with the consequence of contaminating the groundwater.

The temperature in these landfills depends on humidity; as humidity increases, the temperature can go up to 50°C.[2,3] In addition, the temperature increase due to the chemical reactions during the decomposition of organic waste in these landfills has to be considered.[4] This can reach up to 100°C at a depth of $\sim$ 3 m.

Structurally, polyethylene presents very ordered sections, which are responsible for its high degree of crystallinity, as well as disordered sections which account for its amorphous part.

In its crystalline part, the macromolecules are very close together, with strong interactions between neighboring chains, which added to the intramolecular conformational energy, provide the physical and

Correspondence to: F. Avalos-Belmontes (favalos@uadec.edu.mx) or L. F. Ramos-deValle (devalle@ciqa.mx).

chemical stability characteristic of a crystalline structure. On the amorphous part, on the other hand, the macromolecules are arranged at random with relatively weak intermolecular interactions, which render them more susceptible to physical or chemical changes.

For semicrystalline polymers, it is accepted that crystalline and amorphous phases, coexist. One difference among these phases lies in their molecular dynamics. Thermal and X-ray analysis, can characterize these phases; however, their results are limited to information concerning the crystalline phase. In contrast, ^{1}H NMR relaxation analysis enables separate evaluation of crystalline and amorphous molecular dynamics.[5]

It is evident that the films used as geomembranes suffer some degree of ageing along their useful life and it is precisely the oxidative degradation, one of the main considerations to have in mind while establishing its durability.[6] In addition, although normally, polymeric formulations consider the use of antioxidants,[7–10] it must also be considered that the effectiveness of any antioxidant is almost of no use in certain dumping sites where acid or basic environments can be encountered. Hsuan Koerner have reported a very complete study of the half-life time of antioxidants in geomembranes.[11]

In this sense, and considering the results about the elucidation of a polymer lamellar structure via etching,[12–15] it was decided to study the changes taking place in the case a geomembrane gets in contact with a strong acid medium during its useful life.

Considering polyethylene is one of the most used polymers for geomembranes manufacture,[16] it was therefore chosen to carry out this study, and specifically HDPE, due to its well-known structure[17–19] and its mechanical and chemical superiority.

Different spectroscopic techniques have been used to define the amorphous and crystalline sections of PE. Using C-13 NMR, Kitamaru et al.[17] found that samples crystallized from the melt consist of the lamellar crystalline phase, a crystalline-amorphous interphase and an isotropic amorphous phase. Using Fourier transform infrared (FTIR), Kang et al.[20] and Hageman et al.[21] chose the methylene bands between 750 and 700 cm^{-1} to characterize the packing modes of the polyethylene (PE) segments.

The purpose of this work is therefore to study the chemical and morphological changes produced in HDPE when subjecting it to a strong acid attack and to assess the viability of using it in highly demanding applications such as geomembranes.

EXPERIMENTAL

Materials

A commercial HDPE, PADMEX-65050 from PEMEX, with a density of 0.9535 g/cm^3 and a MFR of 6.5 g/10 min was used. Fuming nitric acid was from Merck.

Sample preparation

HDPE pellets were compression molded for 10 min at 160°C to obtain 150 mm × 150 mm × 1 mm plaques from which, 10 mm × 1 mm strips were then cut and put in a fuming nitric acid bath, at 80°C, for different times: 1, 10, 20, 48, 96, and 240 h. In this case, it was decided to use 1-mm thick samples, simply to increase the severity of the tests.

Once extracted from the acid bath, after completing the different treatment times, the samples were washed with distilled water until attaining a neutral pH and finally washed with acetone.

Evaluation

FTIR (Perkin–Elmer Spectrum), with an atenuated total reflectance (ATR) device, was used to determine the chemical changes on the samples, with respect to time of strong acid treatment. The spectra were obtained at 20 scans and resolution of 4 cm^{-1}. Two test specimens were used for each case.

Differential scanning calorimetry (DSC) analysis was performed on a Perkin–Elmer DSC 7 to establish the changes of the thermodynamic variables during treatment in a strong acid medium. All samples, of ca 8 mg were analyzed under a nitrogen atmosphere. The thermal analysis was carried out as follows: the samples were first heated up to fusion (up to 180°C) and then cooled down to 30°C at 10°C/min.

X-ray diffraction (XRD) analysis, for determining the structural changes of samples, was performed in a Siemens D5000 (25 mA, 35 kV) using CuKa X-ray radiation, at 0.68/min, from 1 to 10θ. Samples for X-ray analysis were obtained from the compression molded plaques.

A gel permeation chromatograph V-2000, with a refraction index detector and styragel columns, was used to determine the evolution of molecular weight and molecular weight distribution (MWD) of all samples. These were first dissolved in trichlorobenzene and run in the GPC at 140°C, at a flow rate of 1 mL/min.

To examine the microstructure, samples were taken from the untreated and acid treated strips and coated with Au–Pd for analysis through a Philips Scanning Electron Microscope.

RESULTS AND DISCUSSION

Figure 1 shows the FTIR absorption spectra of the strong acid treated HDPE samples. It can be observed that as time of treatment increases, the characteristic peaks of certain functional groups start to appear. The peak around 1550 cm^{-1} corresponds to NO_2 aliphatic groups, whereas the peak around

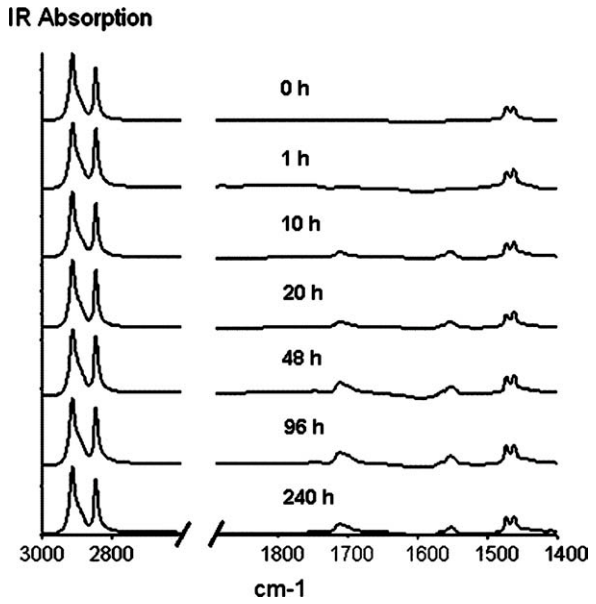

Figure 1 FTIR absorption spectra of HDPE as a function of time of digestion in nitric acid.

1712 cm^{-1} corresponds to carbonyl CO groups.[20,22] There is no evidence of other collateral reaction, nor of branching[23] (889–895 cm^{-1}) or double bonding[24] (909, 990 cm^{-1}, 880 cm^{-1}) that could promote cross-linking.

The appearance of carbonyl groups may be in part due to the breakdown of the polymeric chains. The functionalization and the subsequent chain breakdown occur in the amorphous parts and in the amorphous-crystalline interfaces of polyethylene, which are readily susceptible to the strong acid attack.

Figure 2 presents the variation of the NO_2 and CO absorption indices (A_{1550}/A_{2912} and A_{1712}/A_{2912}), with the time of strong acid treatment. It can be observed that the absorption indices, for these two groups reach a maximum just before 48 h of treatment in the strong acid medium and thereafter, both indices tend to decrease. It may be assumed that this decrease may be because the PE chains get saturated with the NO_2 and CO groups, and considering the polar affinity of the modified PE with the strong acid medium, tend to dissolve in it.

Considering the FTIR results, it can be said that the process of selectively extracting the amorphous phase takes place in two stages. First, there is the chemical modification of the PE chains in the strong acid medium and second, there is the selective dissolution of the modified PE chains.

There are two characteristic IR regions which can be used to follow the PE chain scission, between 2800 and 3000 cm^{-1} and at 1720 cm^{-1}. In the first case, there are the frequencies that correspond to the asymmetric and the symmetric CH_2 vibrations, with peaks at 2927 cm^{-1} and 2855 cm^{-1}, respectively.[25]

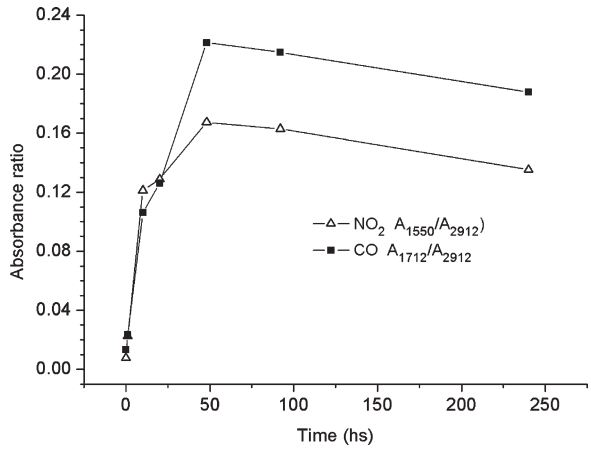

Figure 2 Variation of the infrared absorption index of the NO_2 (A_{1550}/A_{2912}) and CO groups (A_{1712}/A_{2912}) in the HDPE samples as a function of time of digestion in nitric acid.

The one selected in this study was the peak at 2912 cm^{-1}, simply because its absorbance does not exceed the dynamic interval of the instrument used.[26]

The FTIR results explain the process of the PE chain scission which follows the treatment in a strong acid medium. Figure 3 shows that at 1 h of treatment, the chain scission is negligible, as the molecular weight of PE decreases from 128,000 to 120,000 g/mol, though the MWD starts to become slightly bimodal [$\log(M_p) \sim 5$ and $\log(M_p) \sim 4$]. [M_p *represents the molecular weight at the peak of the GPC curve*]. However, at 10 h of treatment, the MW of PE decreases down to a third (45,000 g/mol) and presents a MWD which appears to be trimodal [$\log(M_p) \sim 5$, ~ 4, and ~ 3.5]. In this case, as well as at 20 h of treatment, it appear that precisely the

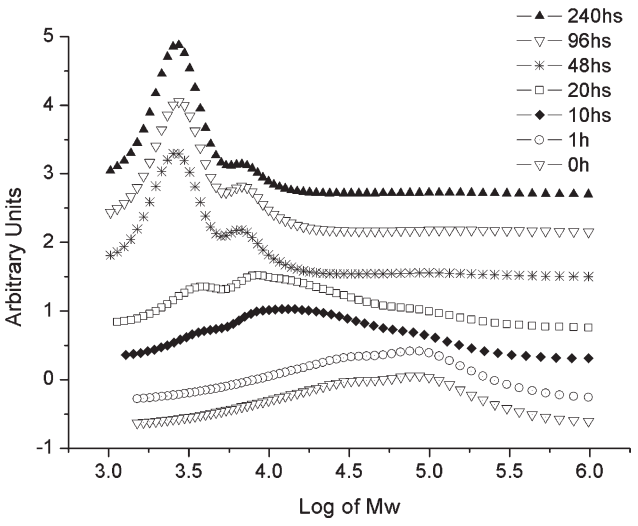

Figure 3 Variation of molecular weight and molecular weight distribution of HDPE samples, as a function of time of digestion in nitric acid.

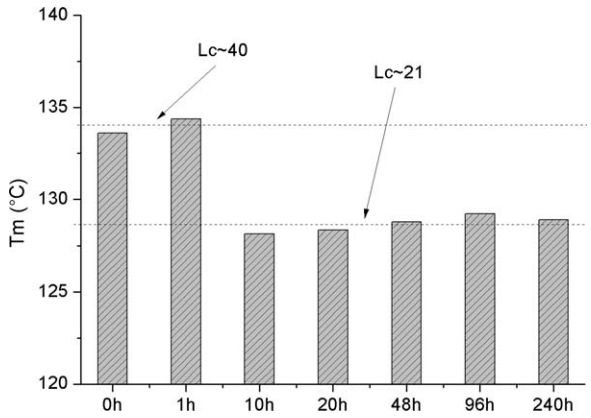

Figure 4 Fusion temperature T_m of HDPE, as a function of time of digestion in nitric acid.

higher molecular weight chains are the ones that tend to scission, down to molecular weights around that of the second maximum of the original multimodal MWD [$\log(M_p) \sim 4$].

At 48 h of treatment the GPC results, Figure 3, show again a bimodal MWD, with well defined peaks around $\log(M_p) \sim 4$ and ~ 3.5, well below the original molecular weights. This is consistent with the FTIR results, where it was shown that the chain scission may in part lead to the formation of COOH and aliphatic NO_2 groups as a product of the oxidative degradation of HDPE.

It can also be observed that as time of treatment increases to 20 h and above, the MWD tends to narrow, with the main peak around $\log(M_p) \sim 3.5$. Above 48 h, the MWD tends to become monomodal, with the peak still around $\log(M_p) \sim 3.5$. Thus, it appears that the PE chain scission going on in this very aggressive acid medium has a limit at around $\log(M_p) \sim 3.5$.

DSC results in Figure 4 show a small increase in the PE T_m at 1 h of treatment, which can be attributed to the chain scission which then raises the local chain mobility, allowing the recrystallization or increase of the crystal perfection, thus increasing the T_m.[27–30]

On the other hand, the later decrease in T_m can be attributed to a decrease in the crystal size, which would result due to occurrence of low MW macromolecules ($\log(M_p) \sim 4$) in the presence of higher MW macromolecules. This would produce the effect of self poisoning, where the low MW species hinder the process of crystal growth.[31]

To assess the structural characteristics of samples as a function of the time of treatment in the strong acid medium, thermodynamic and X-ray reflection[32] determinations were performed. Thus, the crystal thickness (L_c) of the untreated and treated samples was determined after using the Gibbs-Thomson theory as applied to polymers,[33,34] considering the data for HDPE reported elsewhere[35,36] ($T^{\circ}_m = 414.6$ K) and using the melt temperature data (T_m) obtained by DSC in this study; as has been done elsewhere:[37]

$$L_c = 0.627\ T_m^0/(T_m^0 - T_m) \quad (1)$$

The Scherrer equation based in Bragg's law[38] was used for determining the spacing between adjacent crystalline layers (d_{hkl}):

$$d_{hkl} = 0.91\ \lambda/(\beta\ \cos\ \theta) \quad (2)$$

where β is the full width at half-maximum of the diffraction peak in radians, θ is the diffraction angle of the individual peak, and λ is the wavelength of the X-ray.

Even though these two equations are different, the variation of crystal thickness, which is considered in both equations, must be the same.

Examining the results obtained with eqs. (1) and (2) (Fig. 5), the dependency of the crystal size with respect to the homogeneity of the MW can be observed. That is, when the MWD is slightly bimodal and the MW is greater (0–1 h), the crystal thickness is greater, but when the MWD is trimodal and the MW is lesser (10–20 h) the crystal thickness is less. Finally, when the MWD is bimodal and the MW is much lower, the crystal size is the lowest. The larger size as determined via the Gibbs-Thomson theory is because the DSC allows the molecular re-arranging during the sample heating.

The above behavior confirms that the presence of low MW species—guest species—in a world of high MW species—host species—decreases the crystallization rate. The presence of high MW species, on the other hand—now guest species—can cocrystallize

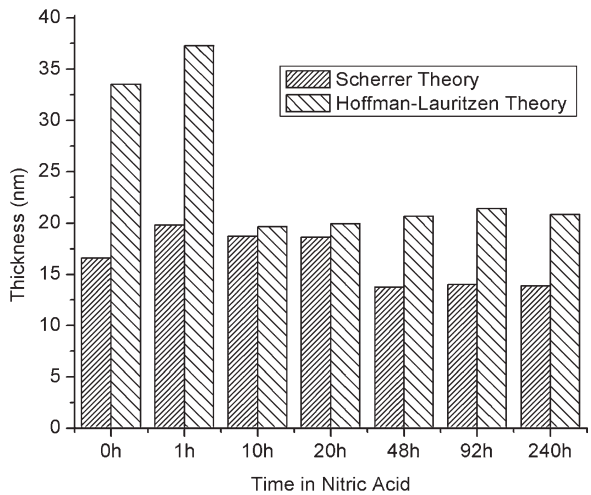

Figure 5 Variation of the crystal size with the time of digestion in nitric acid, and comparison of the crystal size results as obtained by the Scherrer and the Hoffman-Lauritzen theories.

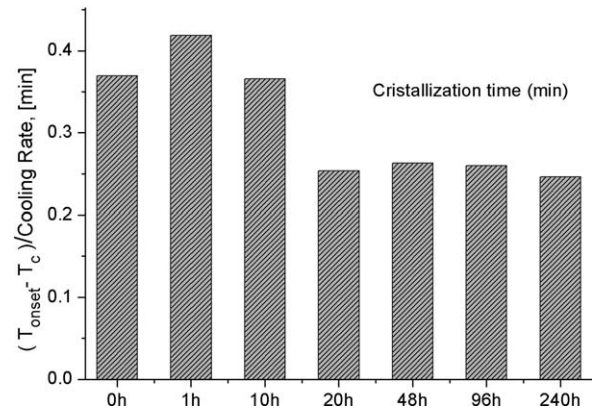

Figure 6 Variation of the crystallization time "($T_{onset} - T_c$)/Cooling Rate" of HDPE, as a function of time of digestion in nitric acid.

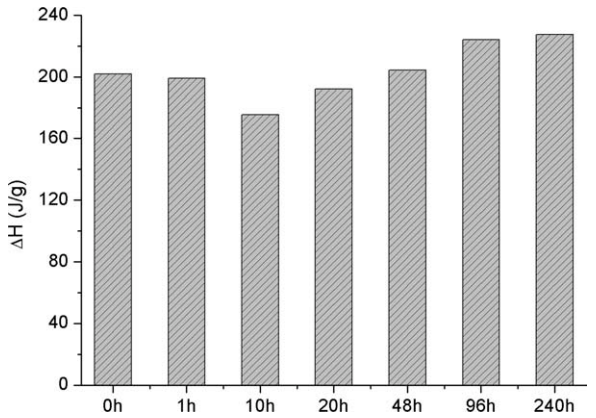

Figure 7 Variation of the enthalpy of crystallization of HDPE, as a function of the time of digestion in nitric acid.

with the low MW species,[39] and this can be corroborated by determining the crystallization time (t_c) through:

$$t_c = (T_{onset} - T_c)/R_c \quad (3)$$

where R_c is the cooling rate in the DSC experiment (°C/min), and T_{onset} and T_c are the temperatures at the onset of crystallization and at the maximum rate of crystallization (at the peak of the crystallization curve).[40] Figure 6 presents the corresponding results.

The above process is also confirmed by the enthalpy of fusion data, presented in Figure 7. In this case, the enthalpy of fusion decreases and reaches a minimum as the time of treatment increases up to 20–48 h, but thereafter, it reverses and increases with the time of treatment. Even above the values of the untreated sample. This decrease in enthalpy during the first hours of treatment is assumed to be because the crystallizable fraction is proportionally less due to the functionalization of the PE molecules as a result of the digestion process. After ~ 10 h of treatment, however, the solvation and extraction of the functionalized molecules begins, and the crystallizable fraction starts to increase.

On the other hand, it can be observed that when the crystal thickness is determined from the XRD data, the variation of d_{hkl} is similar to that of L_c; that is, they both first increase at 1 h of treatment, and then decrease, both reaching a constant value of ca 15 nm. The difference is that at 10 and 20 h of treatment, the values given by the Scherrer equation are still above the initial value and are clearly larger than those given by the Gibbs-Thomson equation.

The initial increase, at 1 h of treatment, may be attributed to the thickening of the crystalline entities due to the rearrangement of the non integer folded

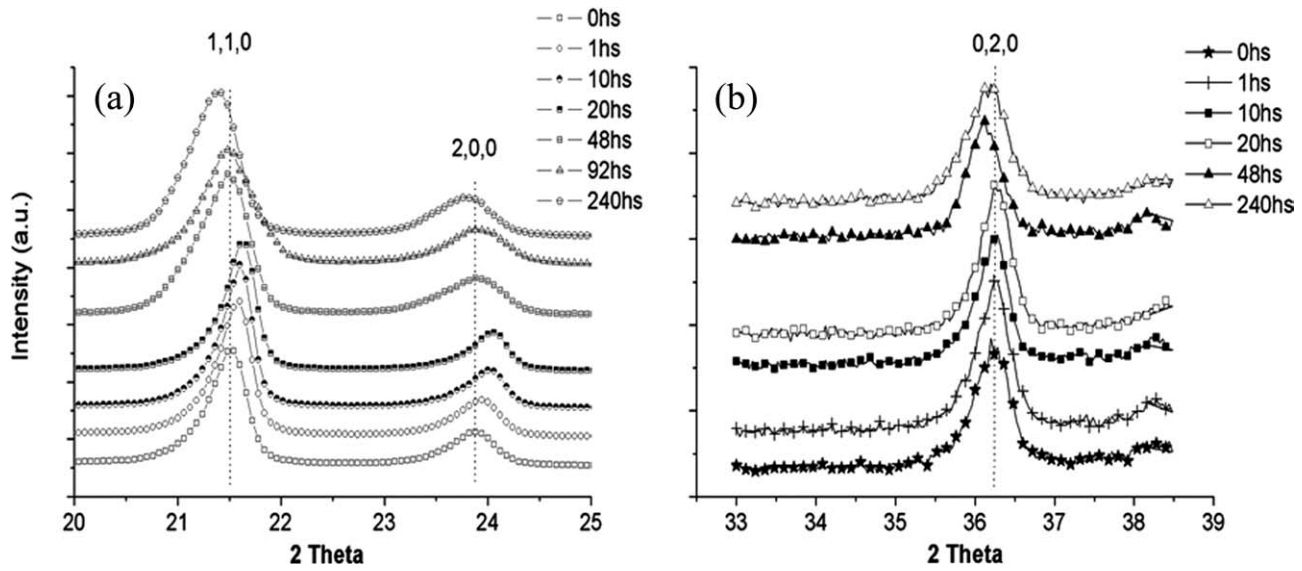

Figure 8 Variation of the peaks corresponding to the crystallographic planes of (110), (200), and (020) of the orthorhombic configuration, as a function of the time of digestion in nitric acid.

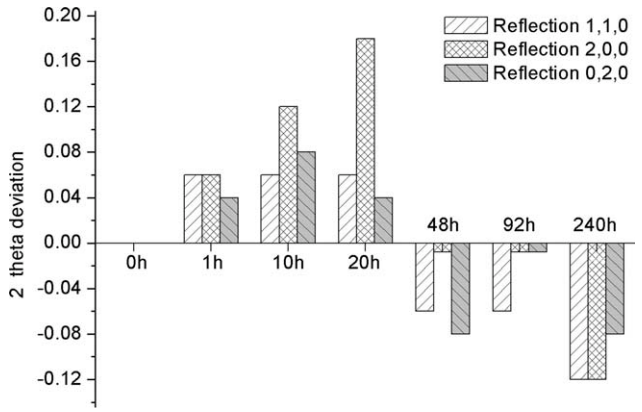

Figure 9 Deviations in the 2θ angle (to lower or higher values), as a function of the time of digestion in nitric acid, as compared with the original HDPE.

chains into the crystal. The differences between predictions of eqs. (1) and (2), specifically at 10 and 20 h of treatment, are related to the trimodal MWD. The intermediate molecular weights [$\log(M_p) \sim 4$] are somehow affecting and producing different data when using the Scherrer equation. Values calculated in this study using the Sherrer equation are in accordance with data reported by other authors using the Bragg's law.[41–43]

Under this consideration, the peaks corresponding to the crystallographic planes of (110), (200), and (020) of the orthorhombic configuration[43–45] are presented in Figure 8. It can be observed that the reflection positions of the treated samples at (200)—*unit cell parameter* ***a***—and (020)—*unit cell parameter* ***b***—deviate with respect to the original HDPE samples.

These deviations occur mostly in the 2,0,0 reflection, especially on samples treated in the strong acid medium for 10 and 20 h, as observed in Figure 9. It is interesting to note that from 0 to 20 h of treatment, this deviation tends to go to higher 2Θ values, but thereafter, the 2Θ value either remains constant or tends to go down again, as compared with the original HDPE samples.

Considering the results by Rizzo et al.[43] these deviations to lower 2Θ angles are due to an increase in the unit cells **a** and **b** and *vice versa*. It can then be assumed that during the first hours of digestion in the strong acid medium, the decrease in the unit cell size is due to the presence of the CO and NO_2 groups that are being generated on the PE chains due to the digestion process. These groups, though not form part of the crystal unit cells, they interfere with the crystallization process and limit the size and perfection of the crystalline unit cells. But thereafter, as the modified PE chains are solvated and washed-out, the remaining unmodified PE chains will tend to produce crystalline structures with less defects and larger dimensions, affecting the crystalline fraction of the sample and the fusion temperature. In samples treated for 10 and 20 h, the greater deviation for the reflection at (200) as compared with that at (020), Figure 9, would correspond to a decrease in the unit cell parameter **a** greater than that of the unit cell parameter **b** in the orthorhombic unit cell of PE.

This could be related to the dependency of the unit cell size with the homogeneity of both, the MWD and the structure. Thus, the trimodal MWD will present much more defects in the unit cell, due to the great variety of molecular weights [$\log(M_p) \sim 5$, ~ 4 and ~ 3.5]. In addition, the presence of groups other than $-CH_2-$ in the amorphous part of the PE might be generating some kind of tensions in the crystalline structure, producing inconsistencies about the crystal thickness.

Examining the DSC and the XRD results, it can be said that the decrease in the enthalpy of fusion of PE as the treatment time increases from zero to 20–48 h, is due to an increase of amorphous sequences along the chains, producing a decrease in the level of crystallinity.

Also, it can be said that the difference between (d_{hkl}) and (L_c), as given by the Scherrer and the Gibbs-Thomson equations, for samples with 10 and 20 h of treatment, is mostly due to an entropy effect. This results from the ample diversity of molecular weights in the samples, which in turn generates many defects in the adjacent crystalline planes resulting in a greater separation of the crystalline lamellas. If the above difference between eqs. (1) and (2) were due to an increase in the unit cell parameters **a** and **b**, this should have coincided with an increase in T_m as obtained from DSC. But the fact is that precisely these samples (those treated for 10 and 20 h) present a slight decrease in T_m, which confirms the presence of smaller size crystal.

CONCLUSIONS

Considering the results presented above, under the severe testing conditions selected as an approximation to the real hazardous conditions in a landfill, it can be concluded that:

The digestion of HDPE in a strong acid medium occurs through chain scission within the amorphous part, which is readily susceptible to the strong acid attack, producing acid groups of the NO_2 y CO type.

The molecular breakdown of HDPE in the strong acid medium produces first, a bimodal MWD with higher molecular weights, followed by a trimodal MWD with intermediate molecular weights, and finally, a bimodal MWD with lower molecular weights.

Apparently, the crystal size is a function of the molecular weight when it is above 10,000 g/mol, but

it is independent when the molecular weight is below this figure.

The oxidation and decrease in molecular weight of the PE would certainly lead to a decrease in the mechanical properties of the geomembrane, which in turn might lead to the geomembrane rupture with the corresponding consequences.

The authors thank CONACYT for its financial support to carry out this study through project 84424. In addition, one of the authors F.A.B. thanks CONACYT for its support to spend a sabbatical at CIQA. Finally, the authors thank M. Sánchez-Adame, M. C. Gonzalez-Cantu, T. Rodriguez-Hernandez, B. Huerta-Martinez, J. Rodriguez-Velazquez, J. F. Zendejo, E. Hurtado-Suarez, and P. Siller-Flores for their valuable technical and informatics support.

References

1. Geomembrane Suppliers; Available at: http://www.power sourcing.com/sg/geomembrane.htm.
2. Koerner, G. R.; Koerner, R. M. J Geotextiles Geomembranes 2006, 24, 129.
3. Rees, J. F. J Chem Technol Biotechnol 1980 30, 458.
4. Crutcher, A. J.; Rovers, F. A. Water, Air, Soil Pollut 1982, 17, 213.
5. Uehara, H.; Aoike, T.; Yamanobe, T.; Komoto, T. Macromolecules 2002, 35, 2640.
6. Dilaraa P. A.; Briassoulis D. J Agricult Eng Res 2000, 76, 309.
7. Morlat-Therias, S.; Fanton, E.; Gardette, J. L.; Tzankova-Dintcheva, N.; La Mantia, F. P.; Malatesta, V. Polym Degrad Stab 2008, 93, 1776.
8. Ponce-Ibarra, V. H.; Benavides, R.; Cadenas-Pliego, G.; Maldonado, H. Polym Degrad Stab 2007, 92, 1133.
9. Wanga, M.; Xua, J.; Wua, H.; Guo, Sh. Polym Degrad Stab 2006, 91, 2101.
10. Ryun-Oh, D.; Hyun-Kyu, K.; Lee, N.; Ho-Chae, K.; Kaang, Sh., Sung-Lee, M.; Hyeon-Kim, T. Bull Korean Chem Soc 2001, 22 629.
11. Hsuan, Y. G.; Koerner, R. M. J Geotech Geoenviron Eng 1998, 124, 532.
12. Palmer R. P., Cobbold A. J. Die Makromol Chemie 1964, 74, 174.
13. Holdsworth, P. J.; Keller, A.; Ward, I. M.; Williams, T. Die Makromolekulare Chemie, 1969, 125, 70.
14. Holdsworth, P. J.; Keller, A. Die Makromolekulare Chemie 1969, 125, 82.
15. Holdsworth, P. J.; Keller, A. Die Makromolekulare Chemie 1969, 125, 94.
16. Müller, W. W. HDPE Geomembranes in Geotechnics; Springer: Berlin, New York, 2007.
17. Kitamaru, R.; Horii, F.; Murayama, K.; Macromolecules 1986, 19, 636.
18. Weeks, N. E.; Mori, S.; Porter, R. S. J Polym Sci Part B Polym Phys 1975, 13, 2031.
19. Weeks, N. E.; Porter, R. S. J Polym Sci Part B-Polym Phys 1975, 13, 2049.
20. Kang, N.; Xu, Y.-Z.; Wu, J.-G.; Feng, W.; Weng, S.-F.; Xu, D.-F. Phys Chem Chem Phys 2000, 2, 3627.
21. Hagemann, H.; Strauss, H. L.; Snyder, R. G. Macromolecules 1987, 20, 2810.
22. Krivoguz, Y. M.; Pesetskii, S. S.; Jurkowski, B. J Appl Polym Sci 2003, 89, 828.
23. Prasad, A. Polym Eng Sci 1998, 38, 1716.
24. Morshedian, J.; Hoseinpour, P. M.; Azizi, H.; Parvizzad, R. Exp Polym Lett 2009, 3, 105.
25. Lu, H.; Hu, Y.; Yang, L.; Wang, Z.; Chen, Z.; Fan, W. J Mater Sci 2005, 40, 43.
26. Bertilsson, A.; Elwing, H.; Liedberg, B.; Larm, O.; Risenfeld, J.; Scholander, E. Mol Eng 1991, 1, 49.
27. Ungar, G., Keller, A. Polymer 1986, 27, 1835.
28. Rastogi, S.; Spoelstra, A. B.; Goossens, J. G. P.; Lemstra, P. J. Macromolecules 1997, 30, 7880.
29. Lee, S. M.; Hye-Jin, J.; Choi, S. W.; Song, H. H. Macromol Res 2006, 14, 640.
30. Lee, S. M.; Choi, S. W.; Nho, Y. C.; Song, H. H. J Polym Sci Polym Phys 2005, 43, 3019.
31. Stephen, W.; Cheng, Z. D.; Lotz, B. Polymer 2005, 46, 8662.
32. Zhang, G.; Watanabe, T. I.; Yoshida, H. Kawai, T. I. Polym J 2003, 35, 173.
33. Hoffman, J. D.; Lauritzen, J. I., Jr. J Res Natl Bur Stand 1961, 65A, 297.
34. Hoffman, J. D.; Weeks, J. J. J Res Natl Bur Stand 1962, 66A, 13.
35. Pak, J.; Wunderlich, B. Macromolecules 2001, 34, 4492.
36. Wunderlich, B.; Czornyj, G. Macromolecules 1977, 10, 906–913.
37. Masirek, R.; Piorkowska, E.; Galeski, A.; Hiltner, A.; Baer, E. Macromolecules 2008, 41, 8086.
38. Bragg, W. L. Proc Camb Phil Soc 1913, 17, 43.
39. Hosier, L.; Bassett, D. C.; Vaughan, A. S. Macromolecules 2000, 33, 8781.
40. Ashraful Islam M., Hussein I., Atiqullah M. Eur Polym J 2007, 43, 599.
41. Ranade, A.; Nayak, K.; Fairbrother, D.; D'Souza, N. A. Polymer 2005, 46, 7323.
42. Liang, G.; Xu, J.; Bao, S.; Xu, W. J Appl Polym Sci 2004, 91, No. 6, 3974–3980.
43. Rizzo, P.; Baione, F.; Guerra, G.; Martinotto, L.; Albizzati, E. Macromolecules 2001, 34, 5175.
44. Fontana, L.; Diep, Q.; Vinh, M.; Santoro, S.; Scandolo, F. A.; Bini, G. R.; Hanfland, M. Phys Rev B 2007, B75, 174112.
45. Lin, Y.; Du, W.; Tu, D.; Zhong, W.; Du, Q. Polym Int 2005, 54, 465.